Growth of a collapsing Langmuir monolayer

S. Kundu, A. Datta, and S. Hazra
Surface Physics Division, Saha Institute of Nuclear Physics, 1/AF Bidhannagar, Kolkata 700064, India
(Received 16 June 2005; revised manuscript received 22 September 2005; published 24 May 2006)

Langmuir monolayers of stearic acid on Co ions in the aqueous subphase have been deposited at different stages of constant pressure collapse, on hydrophilic Si(001) using a modified version of the inverse Langmuir-Schaefer method of horizontal deposition. The electron density profiles (EDPs) along the depth of the deposited films, extracted from the x-ray reflectivity data, show that a monolayer to bi-molecular layer transformation takes place after collapse. The molecules in the lower monolayer have asymmetric configurations with head groups touching water and tails in air, whereas molecules in the upper layer are in symmetric configurations with tails on both sides of the heads. Atomic force microscopy images of the deposited films after collapse, however, show nearly circular islands of height more than that of the bimolecular layer observed in the EDP. As pressure increases, ridges are seen to coexist with these islands. Although the coverage of such islands and ridges is low, they play an important role in determining the growth mode. The growth of the wetting and island layers, taken together, has a striking similarity with the Stranski-Krastanow mode, observed usually for heteroepitaxial growth.

DOI: 10.1103/PhysRevE.73.051608 PACS number(s): 68.18.−g, 68.55.−a, 61.10.Kw, 68.37.Ps

I. INTRODUCTION

Crystalline materials behave elastically up to a certain mechanical stress (called the yield stress [1]) but if the applied stress is more than the yield stress value, plastic deformation occurs. Plastic deformation cannot take place in perfect crystals because this deformation cannot occur without the motion of defects [2]. Before the macroscopic yield stress is reached, microscopic defects and nonelastic deformations take place in the material and ultimately macroscopic flow of dislocations occurs. In two-dimensional systems this plastic deformation leads to a two- to three-dimensional transition, i.e., growth. The deformations created in two dimension cause a plastic flow along the third dimension under mechanical stress and finally form the three-dimensional system. This is a fundamental characteristic of two-dimensional systems as far as the mechanical properties are concerned.

The Langmuir monolayer formed at the air-water interface is a two-dimensional system [3] and shows a two- to three-dimensional transition under overcompression. Under this transition the monolayer shows structural modification perpendicular to and in the plane of the water surface when compressed beyond a critical surface pressure. This critical pressure is called the collapse pressure (π_c) and the newly formed state is called the collapsed state [4]. There are two distinct signatures of collapse in the surface pressure (π)-specific molecular area (A) isotherms. One is a strong spike where a sudden drop of pressure occurs after π_c at a fixed specific molecular area of the monolayer. This is the "constant area collapse." Another is a plateau where pressure is constant after π_c over a certain range of area per molecule. This is the "constant pressure collapse." The isotherm observed in constant pressure collapse can be viewed as an elastic to plastic transformation [5] where the collapse point is the corresponding yield point [1,2]. In the ideal elastic to plastic transformation the stress remains constant for large change in strain [2] but in real monolayer collapse there may be a little deviation. From the observed structural modifications after collapse different mechanisms are proposed by which such collapse can occur. From x-ray studies [6,7] and atomic force microscopy (AFM) analysis [7] of constant pressure collapse it is now established that, at least for fatty-acid Langmuir monolayers on water containing certain divalent metal ions, constant pressure collapse converts the monolayer to a bi-molecular layer. We should note here that fatty-acid molecules interacting with divalent metal ions ultimately produce salts—molecules with two hydrocarbon tails and one metal-bearing head group. These molecules have two obvious configurations shown in (a) and (b) of the inset of Fig. 1. The first (a) is the configuration with the head on one side and the two tails on the other. We shall call this the "asymmetric" configuration. In this configuration the molecules have an amphiphilic nature and can make a stable monolayer on the water surface. We call this monolayer the asymmetric monolayer (AML). The other molecular configuration is shown in the top layer of (b). Here the head is in the

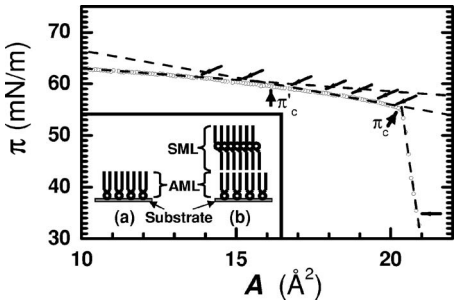

FIG. 1. Surface pressure (π) -specific molecular area (A) isotherms of stearic acid monolayer in presence of cobalt ions in the subphase water at room temperature (24 °C). The curve can be obtained by joining three straight (dashed) lines. The points (π_c and π_c') where slope changes are indicated by thick arrows, while thin arrows indicate the points of film deposition by MILS method. Inset: Model layer(s) on substrate considered for reflectivity analysis: (a) First asymmetric monolayer (AML) and (b) second symmetric monolayer (SML) on first AML.

middle and the two tails are on the two sides. We shall call this the "symmetric" configuration. In this configuration the molecules have a hydrophobic nature and are unstable on the water surface but can make a stable monolayer on a hydrocarbon surface such as oil, a hydrophobic substrate [8], or an AML. The last gives rise to the bimolecular layer observed after collapse [6] or for films of preformed amphiphilic salts on the water surface [9], as shown in (b). We call this stable monolayer of the molecules in symmetric configuration the symmetric monolayer (SML). Of course, the thickness of the SML is twice that of the AML and thus the thickness of the bimolecular layer is three times that of the AML. During constant pressure collapse the mechanical stress (surface pressure) causes the monolayer to buckle. With increase in surface pressure, these buckles transform the molecules from the asymmetric to the symmetric configuration. These can be viewed as permanent "folds" or "defects" in the AML. These folds grow on top of the AML as the compression is increased to form the bimolecular layer.

However, it is still not clear what kind of growth occurs in such plastic deformation. Growth models exist mainly for heteroepitaxial films on solid substrates [10,11]. In these systems the growth mode is governed by the interface and surface energy only. If the sum of the epilayer surface energy (γ_2) and the interface energy (γ_{12}) is less than the surface energy of the substrate (γ_1), i.e., $\gamma_2+\gamma_{12}<\gamma_1$ (wetting condition), the Frank–van der Merwe mode or layer-by-layer growth occurs. If this relation does not hold there is a large excess of surface energy in the growing layer and we have the Volmer-Weber growth mode, i.e., island growth. If, on the other hand, the wetting condition is met, but the upper layer formed in layer-by-layer growth has large strain energy, then isolated islands can form to lower its energy and the Stranski-Krastanow (SK) growth mode, i.e., a wetting layer plus islands, takes place. In homoepitaxial growth, the nucleation density profile of the new Si island on top of a "base" island has been determined [12] and has been compared with homogeneous nucleation theory. This explains this process in the framework of equilibrium step-edge fluctuations and two-dimensional (2D) island ripening. 3D mounds (multilayer stacks of 2D islands) can also be formed in homoepitaxial growth from 2D islands [13]. Besides these, some growth models are also observed for plastic deformation. Hydrogen-induced plastic deformation is observed in Gd thin films where disklike islands and ramp formation are considered [14]. Dislocation patterns are also obtained in metals after plastic deformation [15]. Using atomic force microscopy and scanning white-light interferometry the surface morphology of metals after plastic deformation is being analyzed [16]. But the nature of growth under plastic deformation of two-dimensional systems of soft materials like Langmuir monolayers has not been studied yet.

In the present paper out-of-plane and in-plane structural and morphological features of collapsed films of Langmuir monolayers of stearic acid in the presence of Co ions in water are presented. Collapsed films are deposited on a hydrophilic Si(001) substrate at eight different positions of the π-A isotherm in a modified version of the inverted Langmuir-Schaefer (MILS) technique [6,9]. Analysis of x-ray reflectivity data of all these deposited films gives electron density profiles (EDPs) in the out-of-plane direction from which the out-of-plane structural information is extracted. AFM images give the change in the in-plane morphology of the deposited films after collapse. Also from EDPs and AFM analyses the numbers of molecules in the different layers of the collapsed films are calculated. The combined information extracted from x-ray reflectivity and AFM help to understand the structural evolution after collapse and help to elucidate the growth model under plastic deformation.

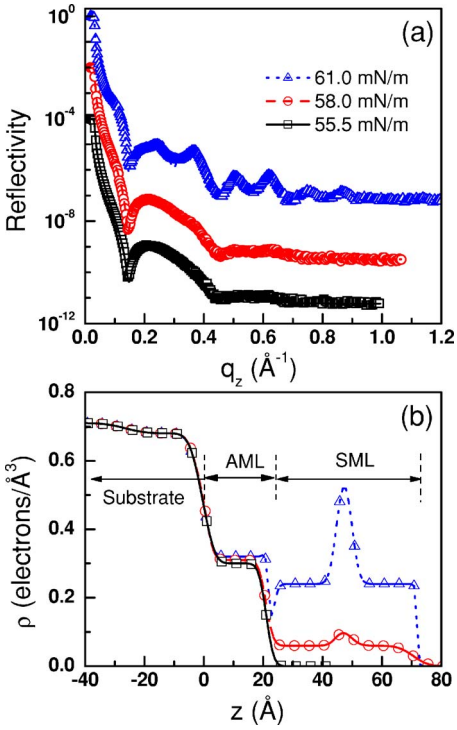

FIG. 2. (Color online) (a) Observed (open symbols) and calculated (lines) x-ray reflectivity profiles of three CoSt films deposited at the different points of the isotherm. Reflectivity profiles and corresponding fits have been shifted vertically for clarity. (b) Electron density profile extracted from reflectivity data corresponding to the model shown in inset of Fig. 1.

II. EXPERIMENTAL DETAILS

Stearic acid (Aldrich, 99.98%) molecules were spread from 200 μl of a 0.56 mg/mL chloroform (Aldrich, 99.98%) solution, in a Langmuir trough (KSV 5000), on Milli-Q water (resistivity 18.2 MΩ cm) containing 0.5 mM $CoCl_2$ (Merck, 98%) at 24 °C. The pH of the subphase water was adjusted by sodium bicarbonate ($NaHCO_3$, Merck, 98%) and was maintained at ~6.5–7.0 at the time of isotherm measurement and film deposition. A platinum Wilhelmy plate was used to measure the surface pressure of the stearic acid monolayer. Stearic acid monolayers were compressed with a speed of 2 mm/min at the time of isotherm measurement and film deposition.

Films of cobalt stearate (CoSt) were deposited on hydrophilic Si(001) substrates. Silicon substrates were made hydrophilic by keeping them in a mixed solution of ammonium

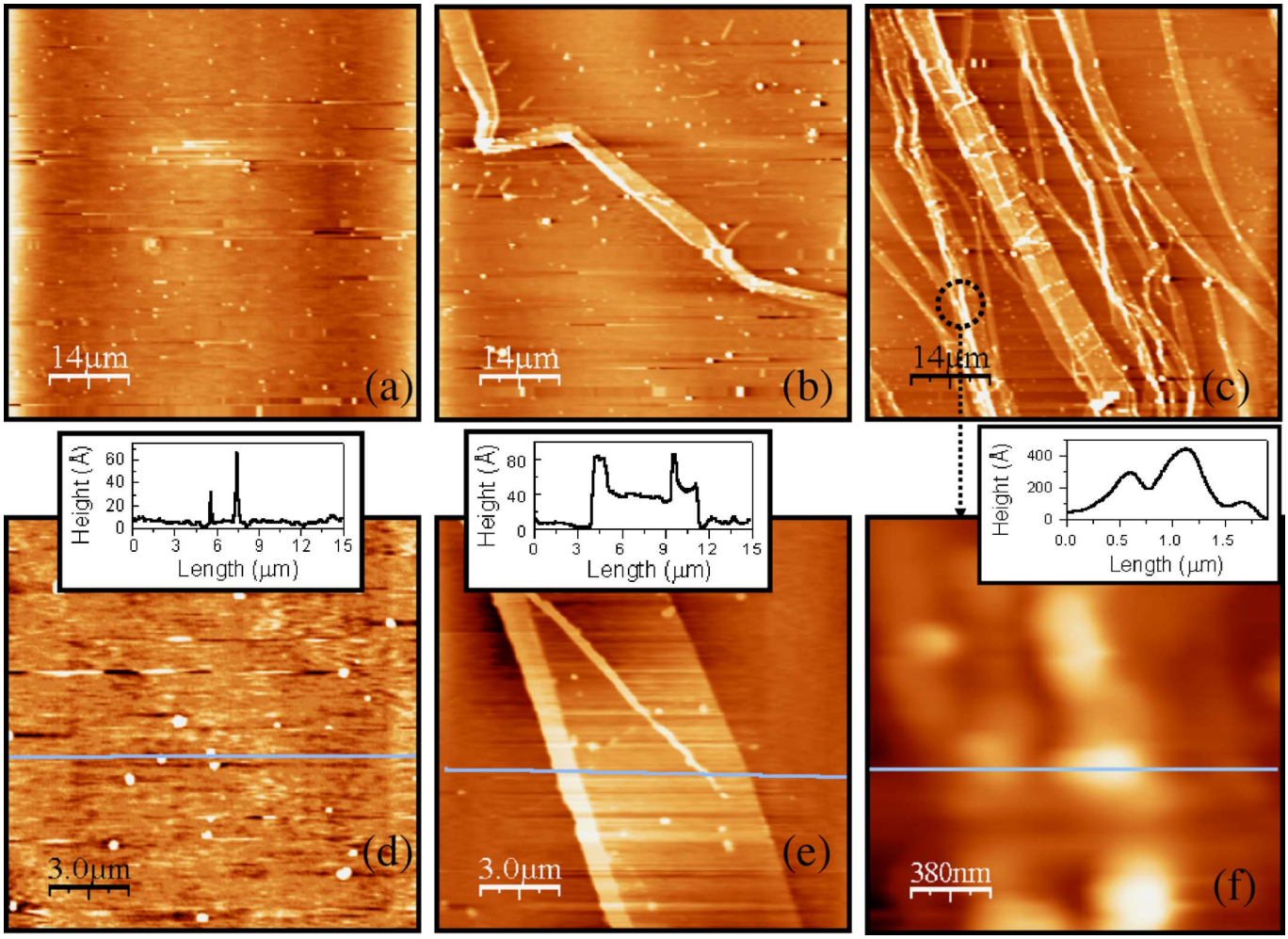

FIG. 3. (Color online) AFM images of the collapsed CoSt films of different scan areas. Scan area (a)–(c) 70×70 μm^2, (d), (e) 15×15 μm^2, and (f) 2×2 μm^2 [zoomed image taken from the area shown by the dotted circle in Fig. 3(c)]. (a) and (d) for film deposited at 56.5 mN/m; (b) and (e) for 58 mN/m; (c) and (f) for 61 mN/m surface pressures. Insets show typical line profiles.

hydroxide (NH_4OH, Merck, 98%), hydrogen peroxide (H_2O_2, Merck 98%) and Milli-Q water (ratio of water, NH_4OH, and H_2O_2=2:1:1 by volume) for 5–10 min at 100 °C. Deposition of the cobalt stearate film by the MILS method has been described previously [6,9]. The hydrophilic silicon substrate was kept horizontally in a home-made L-shaped Teflon substrate holder, which is attached to the clip of the trough dipper and was immersed into water dissolving $CoCl_2$ of 0.5 mM concentration. Stearic acid molecules were spread on the water surface from the same solution (0.5 mg/ml) in the same amount as was spread at the time of isotherm measurement. Depositions were done at eight positions of the isotherm from 35 to 61 mN/m surface pressures (indicated by arrows in Fig. 1) at room temperature (24 °C). The upward speed of the substrate holder was 0.5 mm/min for all depositions, to cause minimum disturbance.

The surface topography of the CoSt films was studied through an AFM (Auto probe CP, Park Scientific) in contact mode using a silicon nitride cantilever (with spring constant 0.05 N/m) and pyramidal tip [17]. Scans were performed in constant force mode over several portions of the film for different scan areas from 5×5 μm^2 to 80×80 μm^2. To minimize the damage to the organic films a low force constant (~0.8 nN) was used. Reflectivity studies of the CoSt films were carried out using an x-ray diffractometer (D8 Discover, Bruker AXS) with Cu source (sealed tube) followed by a Göbel mirror to select and enhance the Cu $K\alpha$ radiation (λ_0=1.54 Å). The diffractometer has a two-circle goniometer [$\theta(\omega)$-2θ] with a $\frac{1}{4}$-circle Eulerian cradle as sample stage. The cradle has two rotational (χ and ϕ) and three translational (X, Y, and Z) motions. The scattered beam was detected using NaI scintillation (point) detector. Measurements were done for ϕ=0°, χ=0°, and varying θ and 2θ in steps of milli-degrees. Instrumental resolution in the out-of-plane direction was 0.0014 $Å^{-1}$. The scattering plane is perpendicular to the sample face. Data were taken in the specular condition, i.e., the incident angle is equal to the exit angle and both are in the scattering plane. Under specular conditions the momentum transfer vector $\boldsymbol{q}=\boldsymbol{k}_f-\boldsymbol{k}_i$ [$\boldsymbol{k}_{i(f)}$ is the incident (scattered) wave vector] has only one nonvanishing component q_z normal to the surface given by $q_z=(4\pi/\lambda)\sin\theta$, where θ is the angle the incident x-ray beam makes with the surface [17,18].

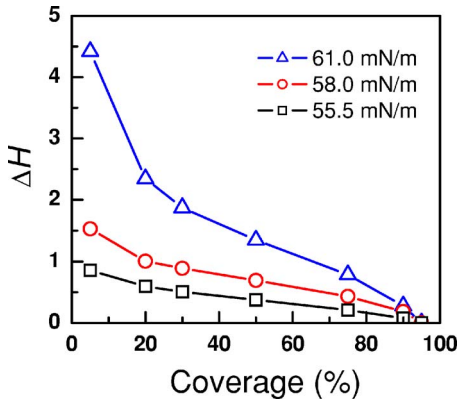

FIG. 4. (Color online) Heights (ΔH, in units of AML thickness) above base as a function of bearing ratio or coverage obtained from AFM images for CoSt films deposited at the different points of the isotherm.

III. RESULTS AND DISCUSSION

A. Isotherm studies

Surface pressure (π)-specific molecular area (A) isotherms of a stearic acid monolayer in the presence of cobalt ions in the subphase water were taken at room temperature and a typical isotherm is shown in Fig. 1. Constant pressure collapse was observed for a CoSt monolayer in water at pH 6.5–7.0. The π_c was 55 mN/m and was independent of the compression rate [6]. Films were deposited by the MILS method at the eight points indicated by arrows. One deposition point was at 35 mN/m, i.e., far before collapse. The other seven points at which films were deposited were at 55.5, 56.5, 57.3, 58, 59, 60, and 61 mN/m surface pressures. Three straight lines can represent the isotherm presented in Fig. 1, with changes in slope at π_c and π_c' indicated by thick arrows.

B. Microscopic considerations

The most important general concept used to analyze the microscopic data (x-ray scattering and AFM) is the presence of molecules with two different linear dimensions, one (symmetric) being twice the other (asymmetric). We have measured the thickness and height in units of the AML to have the same unit throughout and to have no fractional heights. But the same concept cannot be used for coverage, density, or surface density, since energy considerations dictate that, above the first monolayer, which is an AML, all other layers ought to be SMLs, and such layers by definition cannot be described as coverages of two AMLs, one on top of the other. Hence for the first layer we use AML coverage and for all subsequent layers, including incomplete layers or islands, we use SML coverage.

C. X-ray reflectivity studies

X-ray reflectivity data of all the eight samples were taken and analysis was done by the Parratt formalism [18] introducing a finite interfacial width [19]. X-ray reflectivity data of three typical films are shown in Fig. 2(a). All other data

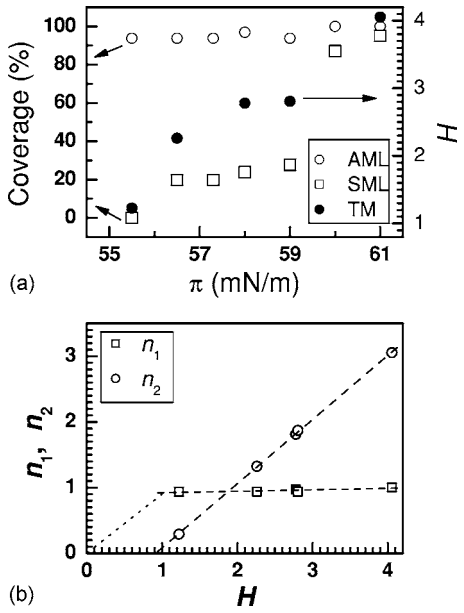

FIG. 5. (a) Coverage of wetting AML and islands of SML for the deposited films obtained from x-ray reflectivity as function of surface pressure. The total molecules (TM) in units of AML thickness (H) deposited in the films, obtained from both x-ray reflectivity and AFM measurements as a function of surface pressure is also included. (b) Wetting layer thickness (n_1) and island forming layer thickness (n_2) as a function of the total deposited molecules (H). All are in units of AML. Dashed lines are straight lines passing through experimental points, while the dotted straight line is the expected variation of the wetting layer before collapse predicted from known monolayer behavior.

are close to one of these three classes and therefore are not presented. Reflectivity data obtained from all the films were analyzed using a bimolecular layer model consisting of the AML+SML [6] shown in the inset of Fig. 1. The calculated reflectivity curves for the best fits are presented in Fig. 2(a) with the corresponding EDPs in Fig. 2(b). From the values of the electron densities of the individual layer we can calculate the coverage of each layer. For the hydrocarbon tails, the electron density of 0.32 electrons/Å^3 corresponds to 100% coverage. The EDPs of Fig. 2(b) show that the film deposited at π=55.5 mN/m consists of a single AML with nearly 100% coverage, the film deposited at π=58.0 mN/m has an AML with nearly 100% and one SML of ~28% coverage, while the film deposited at π=61 mN/m is made of an AML and a SML, both having nearly 100% coverage.

D. AFM studies

AFM images depicting the surface topography of all the collapsed cobalt stearate films are shown in Fig. 3. Broad features of the samples are clear from the large area (70×70 μm^2) scans as shown in the upper panel of this figure. For the film deposited at 56.5 mN/m surface pressure, there is almost no information except some small but circular islands, while for the film deposited at 58 mN/m surface pressure, the beginnings of ridgelike patterns are evident coexisting with the same islandlike patterns. Such ridge-

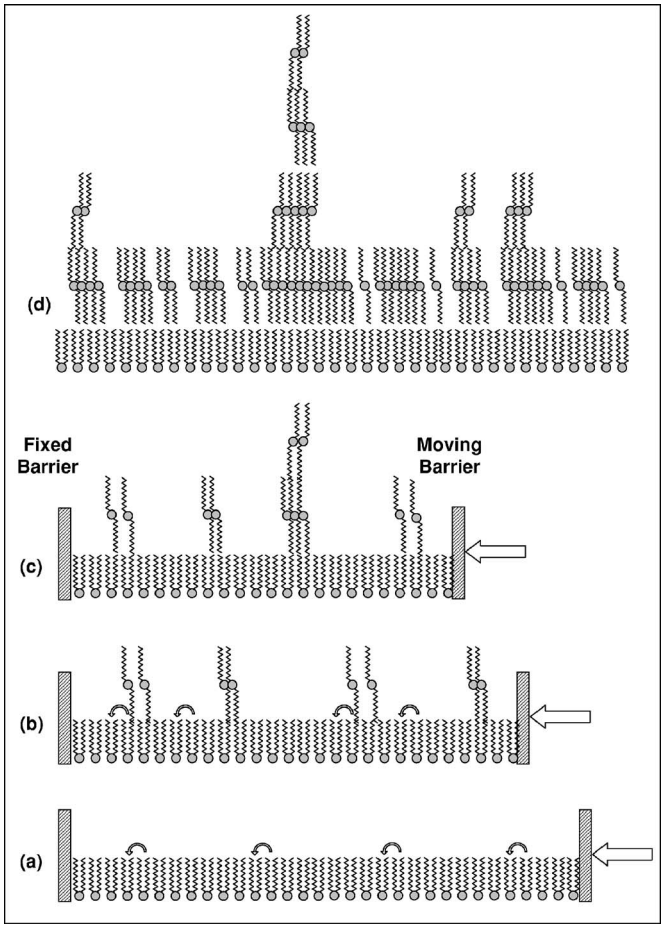

FIG. 6. Schematic illustration of collapsing Langmuir monolayer growth behavior. (a) Wetting monolayer with full coverage just before collapse. (b) Islands of symmetric monolayer thickness start to form by flipping up some molecules from the wetting monolayer at random positions to release the excess pressure due to barrier compression. (c) Islands of multiple bilayer thickness form by same flipping up of molecules from the wetting monolayer by further compression. (d) Final structure of the collapsing film with wetting layer of asymmetric monolayer thickness and island layer having thickness in multiples of SML, but predominantly of one SML.

like patterns increase considerably for the film deposited at 61 mN/m. Ridges form mostly perpendicular to the compression direction, i.e., parallel to the barrier, but branches are also present. The lower panel shows small area [for Figs. 3(d) and 3(e) scan area is 15×15 μm^2 and for Fig. 3(f) scan area is 2×2 μm^2] scans to illustrate detailed features. From these high magnification images we suggest that the ridges may be collections of small islands. The islands start appearing consistently at the same point of compression, thus ruling out their origin from contaminants.

Why do these islands or ridges not show up in the EDPs extracted from the x-ray scattering data? To answer this we have plotted in Fig. 4 the islands or ridges of minimum height (ΔH, in units of AML thickness) above base as a function of the coverage for different films, which is obtained from the bearing ratio [20]. The bearing ratio is essentially an integral of the height histogram from the top surface, i.e., a plot of percentage of data points at or above a given height that we have taken as base. For the films deposited at $\pi=55.5$ and 58.0 mN/m, this "base" is the AML but at $\pi=61$ mN/m, it is the AML plus one SML. ΔH is ideally integer in number but experimentally fractional because the geometry effect of the tip is convoluted with the actual height of the layers. Figure 4 provides the amount of coverage of islands and ridges having height ΔH or more above the corresponding base layer. We find that there is a jump in the coverages by islands and ridges of all heights for the film deposited at $\pi=61$ mN/m. More important, however, is the fact that even for that film, islands and ridges with one SML thickness above its base, i.e., two SMLs above the AML, have a coverage $\leqslant20\%$ and this coverage becomes almost negligible for thickness of three SMLs or above. The low coverage of islands and ridges having thickness more than one SML is the reason for them to be undetected by x rays. Nevertheless, these features are very important in understanding the growth mode, as we will see in the next section.

E. Growth model

Coverages of AMLs and SMLs in the films obtained from their EDPs are plotted in Fig. 5(a) versus the deposition surface pressure. The AML coverage is found to be almost 100% in all the films, while SML coverage increases nonlinearly. For films deposited at $\pi=56.5-59.0$ mN/m the SML coverage is about 20–28 %. But for the film deposited at $\pi=60$ mN/m, there is a sudden jump of SML coverage to $\sim87\%$ and then there is a gradual increase for the next higher surface pressure. To understand this sudden jump we have calculated the total number of molecules (TM) transferred in the films, using both x-ray and AFM results. The TM, in units of AML thickness (H), is also plotted in Fig. 5(a) versus deposition surface pressure. A similar jump at the same position is evident, which suggests a sudden high transfer of molecules per unit area. Although the reason for such a high transfer is not clear it can be assumed generally that the movement of the barrier causes some molecules in the monolayer to flip up to the SML and some to dissolve in water. The increase in the number of molecules we observe is due to those flip ups. At the point of surface pressure where jump occurs, it seems that dissolution in water becomes negligible and most of the molecules are taken to the SMLs by the barrier movement. This is also suggested by the lowering of $\partial\pi/\partial A$, as indicated by the slopes of the dashed lines, in the isotherm at $\pi_c'\cong59$ mN/m (Fig. 1). If this is indeed the reason behind the observed increase in coverage by the symmetric molecules, it clearly indicates that the asymmetric to symmetric transformation is the preferred mechanism to release stress due to compression by barrier movement. However, more definitive studies are required to clarify this issue.

In order to understand the growth mode during constant pressure Langmuir monolayer collapse it is useful to plot the AML number density and island layer (composed of islands and ridges of SMLs) number density as functions of the number density of total molecules. These have been calculated from the EDP and the bearing ratio, the former giving

the electron densities and the latter giving the volumes, from which we have derived the number density of each layer. Here the number of molecules per unit area with full coverage in a monolayer is considered to be the unit number density. For full coverage, 20 $Å^2$ is taken to be the area per molecule [21]. The number densities of the AML (n_1) and the island layer (n_2) plotted against the number density of total molecules ($H=n_1+n_2$) are shown in Fig. 5(b), where n_1 is calculated from x-ray reflectivity results while n_2 and H have been calculated using both x-ray and AFM results. Straight lines nicely fit both data. It is seen that n_1 is almost constant, which corresponds to a "wetting layer" with full coverage, while the island layer (composed of islands and ridges) increases linearly with total molecule density. These features of "growth" of a collapsing Langmuir monolayer have a strong resemblance to the SK-type growth mode [10,11] generally observed for heteroepitaxial systems.

We are proposing the following model for the process of growth due to collapse of the Langmuir monolayer in terms of cobalt stearate molecules in the two configurations we described. Initially, i.e., below collapse pressure, the system consists of only one monolayer of molecules in the asymmetric configuration. The coverage of this layer, which is obtained from the surface number density of these molecules, increases to nearly 100% just before collapse as can be predicted from the isotherm as well as the known Langmuir monolayer behavior [3,4,21]. This is indicated by the dotted line in Fig. 5(b). This layer we are calling the wetting layer and it is schematically depicted in Fig. 6(a). It should be remembered here that wetting and nonwetting in our system are with reference to water and, unlike the classical SK model, while the AML wets water completely, the SML is completely nonwetting. Beyond collapse pressure, some of the asymmetrically configured molecules are converted to the symmetric configuration. Since these cannot stay on water they go up on the wetting layer and this process would go on to create a complete SML on the AML. However, from the point of view of energy minimization, the top of the AML or of any SML is equivalent to molecules in the symmetric configuration. In Fig. 6(b) SMLs are shown to indicate the existence of islands after compression of the barrier, whereas in Figs. 6(c) and 6(d) the coexistence of islands and ridges is shown with further barrier compression. Here we want to point out that the islands and ridges are two morphological features of basically multiples of SMLs that are collected differently in the in-plane direction. For islands they are few in number while for ridges they are large in numbers, forming wide stripes that are visible in the AFM images. Hence, there will be growth of islands and ridges of these molecules along with the growth of this SML, though we are not sure about the details of this island layer growth. The height of the ridges as well islands above the wetting layer will be in multiples of the linear dimension of the symmetrically configured molecule, i.e., the SML thickness, and the coverage will also be in terms of the number density of these molecules. Thus, though the reason behind the coexistence of islands and layers in a standard SK growth process is different from that in our system, the results look the same and suggest a generalization of the growth mode.

IV. CONCLUSIONS

From x-ray reflectivity and AFM images of films transferred to Si substrates by horizontal deposition we have extracted the structure and morphology of stearic acid Langmuir monolayers in the presence of Co ions in the aqueous subphase, at different stages after constant pressure collapse, and there from we have tried to understand the nature of growth in the third dimension under such plastic deformation. X-ray reflectivity analysis shows that a monolayer with molecules in the asymmetric configuration, considered as the wetting layer, formed on water, is also transferred to the substrate. After collapse, islands of molecules in the symmetric configuration form on this complete wetting layer, the coverage of which increases with pressure. From AFM topography it is evident that islands of multiple layers of the symmetrically configured molecules are also formed, although they are too small to affect the x-ray reflectivity analysis. With further plastic deformation nearly parallel high ridges are formed along with these islands. The growth of the wetting and island layers, taken together, has a striking similarity with the Stranski-Krastanow heteroepitaxial growth mode, indicating the presence of simultaneous and competing growth mechanisms. These results are thus important for two- to three-dimensional transitions in general, where such competing interactions are present.

[1] A. E. H. Love, *A Treatise on the Mathematical Theory of Elasticity* (Dover Publications, New York, 1927).
[2] I. Kovács and L. Zsoldos, *Dislocations and Plastic Deformation* (Pergamon Press, Oxford, 1973).
[3] M. C. Petty, *Langmuir-Blodgett Films: An Introduction* (Cambridge University Press, Cambridge, U.K., 1996).
[4] G. L. Gaines, *Insoluble Monolayers at Liquid-Gas Interfaces* (Interscience, New York, 1966).
[5] J. P. Kampf, C. W. Frank, E. E. Malmstörm, and C. J. Hawker, Science **283**, 1730 (1999).
[6] S. Kundu, A. Datta, and S. Hazra, Langmuir **21**, 5894 (2005).
[7] C. Gourier, C. M. Knobler, J. Daillant, and D. Chatenay, Langmuir **18**, 9434 (2002).
[8] M. K. Mukhopadhyay, M. K. Sanyal, A. Datta, J. Webster, and J. Penfold, Chem. Phys. Lett. **407**, 276 (2005).
[9] A. Datta, S. Kundu, M. K. Sanyal, J. Daillant, D. Luzet, C. Blot, and B. Struth, Phys. Rev. E **71**, 041604 (2005).
[10] I. Daruka and A.-L. Barabási, Phys. Rev. Lett. **79**, 3708 (1997).
[11] V. A. Shchukin and D. Bimberg, Rev. Mod. Phys. **71**, 1125 (1999).
[12] W. Theis and R. M. Tromp, Phys. Rev. Lett. **76**, 2770 (1996).
[13] K. J. Caspersen, A. R. Layson, C. R. Stoldt, V. Fournee, P. A. Thiel, and J. W. Evans, Phys. Rev. B **65**, 193407 (2002).

[14] A. Pundt, M. Getzlaff, M. Bode, R. Kirchheim, and R. Wiesendanger, Phys. Rev. B **61**, 9964 (2000).
[15] P. Hähner, K. Bay, and M. Zaiser, Phys. Rev. Lett. **81**, 2470 (1998).
[16] M. Zaiser, F. M. Grassett, V. Koutsos, and E. C. Aifantis, Phys. Rev. Lett. **93**, 195507 (2004).
[17] J. K. Basu, S. Hazra, and M. K. Sanyal, Phys. Rev. Lett. **82**, 4675 (1999).
[18] L. G. Parratt, Phys. Rev. **95**, 359 (1954); J. K. Basu and M. K. Sanyal, Phys. Rep. **363**, 1 (2002).
[19] J. Daillant and A. Gibaud, *X-Ray and Neutron Reflectivity: Principles and Applications* (Springer, Berlin, 1999); M. Tolan, *X-Ray Scattering from Soft Matter Thin Films* (Springer, Berlin, 1999).
[20] S. Kundu, S. Hazra, S. Banerjee, M. K. Sanyal, S. K. Mandal, S. Chaudhuri, and A. K. Pal, J. Phys. D **31**, L73 (1998),.
[21] V. M. Kaganer, H. Möhwald, and P. Dutta, Rev. Mod. Phys. **71**, 779 (1999).